PROCEEDINGS REPRINT

SPIE–The International Society for Optical Engineering

Reprinted from

CSNO '93 International Workshop

Computer Simulation in Nonlinear Optics

27 June–4 July 1993
Moscow–Nizhny Novgorod

SPIE P PROCEEDINGS SERIES

Volume 2098

A simulation approach to Fokker-Planck modelling of lasers and optical amplifiers

G. M. D'Ariano and C. Macchiavello

Dipartimento di Fisica 'Alessandro Volta', via Bassi 6, I-27100 Pavia, Italy

ABSTRACT

We present a novel numerical method to solve Fokker-Planck equations in quantum optics, based on a Monte Carlo simulation of the probability diffusion process. The method is especially useful for multimode analysis, and hence for studying realistic models of nonlinear optical systems. Two simple examples are given: the first is a one-dimensional Fokker-Planck equation in the number representation, which describes a simple model of optical amplifier; the second is a two-dimensional equation in the P-function representation—the quasi-probability for normal-ordered averages—which corresponds to the customary Van der Pol model of the laser threshold. In this case also the field correlation function and spectrum are numerically simulated.

1. INTRODUCTION

Simulation methods have been recently introduced in quantum optics and proved to be very efficient for treating complex nonlinear systems. In Refs. [1] a Monte Carlo wave function method has been developed which allows the solution of the master equation. The master equation approach, however, is not suited to large numbers of photons, which determine the effective dimension of the truncated Hilbert space. This is an often encountered case in practical situations, as for example when studying lasers or optical amplifiers. Here the Fokker-Planck equation is a more suited tool for numerical evaluations. Depending on the analytical form of the drift and diffusion matrices, it can model a wide class of phenomenology in quantum optics, also allowing a precise treatment of the noise of quantum origin in presence of saturation—and, more generally, nonlinear—effects[2]. Apart from the case of very small numbers of photons, the Fokker-Planck equation is thus suited to treat any range of radiation intensity.

In this paper we show a novel simulation method to solve the Fokker-Planck equation. As in the case of any statistical integration method, the present approach is particularly useful—especially for time-consuming—when a multidimensional (i.e. multimode) analysis is concerned. The main ingredient is simply the Monte Carlo simulation of the Green-function solution for infinitesimal time steps. On the basis of some examples we illustrate the large potentialities of the method in studying concrete complex models in quantum optics.

-8194-1381-X/94/$6.00

2. OUTLINE OF THE METHOD

The Fokker-Planck equation in its most general form is

$$\partial_t P(\mathbf{x},t) = -\nabla_{\mathbf{x}} \cdot [\mathbf{Q}(\mathbf{x})P(\mathbf{x},t)] + \frac{1}{2}\nabla_{\mathbf{x}}\nabla_{\mathbf{x}} : [\mathbf{D}(\mathbf{x})P(\mathbf{x},t)] \, . \tag{1}$$

In Eq. (1) $P(\mathbf{x},t)$ is a probability (or quasi-probability) distribution in the d-dimensional space of the vectors $\mathbf{x} \in \mathbf{R}^d$, $\mathbf{Q}(\mathbf{x})$ is the drift vector, and $\mathbf{D}(\mathbf{x})$ is the diffusion matrix. For example, $\mathbf{x}$ can represent a set of photon numbers for different modes of radiation, but also a set of complex field amplitudes in $\mathbf{C}^d \equiv \mathbf{R}^{2d}$: the former case corresponds to a number representation probability distribution, the latter to a Wigner-function (quasi)-probability. Notice that the present method needs to consider only the case of positive definite $P(\mathbf{x},t)$. For the more general case of non positive definite probabilities, as, for example, the normal-ordering P-function, the problem can still be faced when both initial condition and diffusion matrix ensure a positive definite probability for all times. An example of such an application is given in the followings.

The Green-function of Eq. (1) for an "infinitesimal" evolution time Δt—or for a finite Δt, but constant drift and diffusion—has the Gaussian form

$$G(\mathbf{x},\mathbf{x}';\Delta t) = \left(\det \mathbf{D}(2\pi\Delta t)^d\right)^{-1/2} \exp\left[-(\mathbf{x}'-\mathbf{x}+\mathbf{Q}\Delta t)\cdot(2\Delta t\mathbf{D})^{-1}\cdot(\mathbf{x}'-\mathbf{x}+\mathbf{Q}\Delta t)\right] \, . \tag{2}$$

The Green-function (2) is the solution of Eq. (1) for initial condition $P(\mathbf{x},0) = \delta(\mathbf{x}-\mathbf{x}')$. The evolution of the probability distribution for short times is

$$P(\mathbf{x},t+\Delta t) = \int_{\mathbf{R}^d} d\mathbf{x}' G(\mathbf{x},\mathbf{x}';\Delta t)P(\mathbf{x}',t) \, . \tag{3}$$

The integration (3) becomes very time-consuming—in practice, prohibitive—already for dimensions $d \geq 2$. The Monte Carlo method avoids the problem of integration (3) upon simulating the evolution of the probability for each point $\mathbf{x}$, according to the Gaussian process represented by the Green-function itself in Eq. (2). This only needs a statistical sampling of the initial probability distribution, which can be obtained by standard Metropolis algorithms.

Following the above indications, we describe the probability $P(\mathbf{x},t)$ for a generic time t by means of a statistical ensemble of N events/points $\{\mathbf{x}_1(t),\mathbf{x}_2(t),\ldots,\mathbf{x}_N(t)\}$, which are step-by-step time-evolved as

$$\mathbf{x}_i(t+\Delta t) = \mathbf{x}_i(t) + \mathbf{Q}(\mathbf{x}_i(t))\Delta t + \mathbf{E}(t) \, , \tag{4}$$

where $\mathbf{E}(t)$ is a zero-average Gaussian process with variance $\mathbf{D}(\mathbf{x}_i(t))\Delta t$. The quantities of interest are statistically evaluated on the ensemble as usual

$$\overline{F(t)} \equiv \frac{1}{N}\sum_{i=1}^{N} F(\mathbf{x}_i(t)) \, . \tag{5}$$

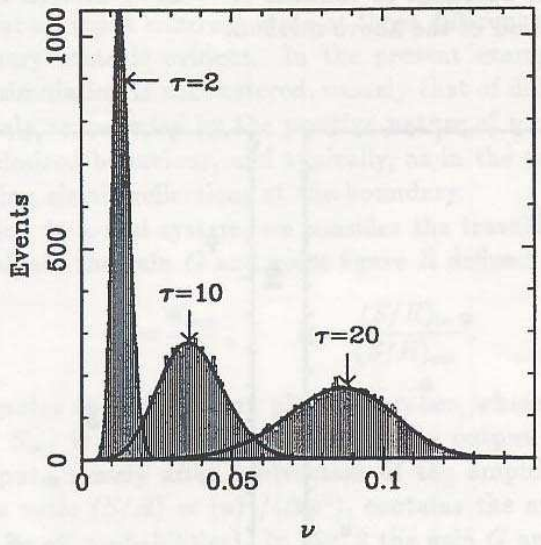

Figure 1: Histograms representing the evolution of the probability distribution at τ =2, 10, and 20, for the one-dimensional Fokker-Planck equation with drift and diffusion coefficients given in Eqs.(8,9). Here $n_* = 10^4$, $\theta = 1.15$, and $\bar{n} = \theta' = 0$. At $\tau = 0$ an input coherent state has been used with $\langle \hat{n} \rangle_0 = 100$. The full line represents the result from direct numerical integration.

For $N \to \infty$ the central-limit theorem ensures that

$$\lim_{N\to\infty} \frac{1}{N} \sum_{i=1}^{N} F(\mathbf{x}_i(t)) = \int F(\mathbf{x}) P(\mathbf{x}, t) d\mathbf{x} \equiv \langle F(t) \rangle \,, \tag{6}$$

and for finite N the estimation of the error on the average is

$$\Delta F(t) \simeq \sqrt{\frac{\sigma_F^2(t)}{N}} = \sqrt{\frac{\overline{F(t)^2} - \overline{F(t)}^2}{N}} \,, \tag{7}$$

which is a decreasing function of N, independently on the dimension of the configuration space (this should be compared with the number of steps needed for convergence of customary integration algorithms, which is an exponentially increasing function of the dimension d). Eq. (7) also allows a self-consistent check of the whole procedure. The only remaining source of (systematic) errors is, in practice, the choice of the time step Δt, which has to be tuned short enough to satisfy Eq. (2), depending on the particular form of the diffusion and drift coefficients (typically, at fixed Δt, one has larger systematic

errors for increasing order of the evaluated distribution moment). On the other hand, it is not necessary to use very large statistical ensembles, and in order to obtain reasonable estimated error-bars it is sufficient to consider $N \sim 10^4 \div 10^5$. In the following we give two examples of application of the above method.

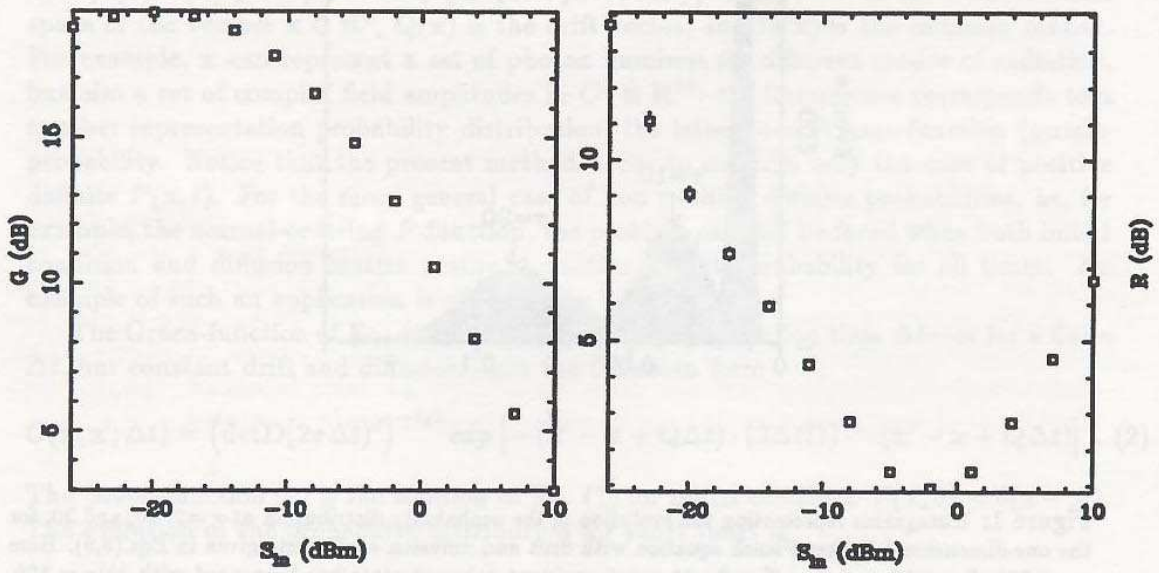

Figure 2: Gain G and noise figure F for the travelling wave optical amplifier of Ref. [5], as a function of the input power.

3. APPLICATION TO A SIMPLE TWOA MODEL

In this first example we consider the Fokker-Planck equation which can be derived from the laser one-mode master equation of Ref.[4] in the limit of large photon saturation numbers. The probability distribution $P(\nu,\tau)$ describes the evolution of the normalized photon number $\nu = \frac{n}{n_*}$ for saturation number n_*, and with τ being the time rescaled by the cavity damping time. The drift and diffusion coefficients have the simple form

$$Q(\nu) = (\nu + n_*^{-1})\left[\bar{n} + \theta(1+\nu+n_*^{-1})^{-1}\right] - \nu\left[1+\bar{n}+\theta'(1+\nu)^{-1}\right] , \quad (8)$$

$$D(\nu) = \frac{1}{2n_*}\left\{(\nu + n_*^{-1})\left[\bar{n} + \theta(1+\nu+n_*^{-1})^{-1}\right] + \nu\left[1+\bar{n}+\theta'(1+\nu)^{-1}\right]\right\} , \quad (9)$$

where $\bar{n}$ is the thermal photon number, whereas θ and θ' are pumping parameters which are proportional to the injection rates of atoms in the excited and ground state

respectively. The present simple model is suited also to describe a travelling wave optical amplifier or, equivalently, an active fibre amplifier for negligible depletion of the pumping radiation mode. A sample of the probability evolution is given in Fig. 1, where the function $P(\nu,\tau)$ is plotted for an input coherent state at three different values of τ. The approach toward the stationary state is evident. In the present example, a typical problem of diffusion equation simulation is encountered, namely that of diffusion beyond the domain boundaries, here only represented by the positive nature of ν. There are many methods to handle such undesired behaviour, and typically, as in the present case, a suited trick consists in simulating elastic reflections at the boundary.

As an application to a real system, we consider the travelling wave optical amplifier of Ref. [5]. We evaluate the gain G and noise figure R defined as follows

$$G = \frac{S_{out}}{S_{in}}\,, \qquad R = \frac{(S/R)_{in}}{(S/R)_{out}}\,. \tag{10}$$

In Eq. (10) S_{in} denotes the input mean photon number, whereas, for on-off modulation, the output signal S_{out} is the difference between the output mean values in presence and absence of input, namely after subtraction of the amplified spontaneous emission (the signal-to-noise ratio $(S/R) = \langle n\rangle^2/\langle\Delta n^2\rangle$, contains the number fluctuations $\langle\Delta n^2\rangle$ averaged on equal on-off probabilities). In Fig. 2 the gain G and noise figure R obtained from a numerical simulation are plotted. These results can be compared with those reported in Ref. [5], where, however, the amplified spontaneous emission has not been subtracted, leading to (unphysical) minimum noise figures lower than unit.

4. APPLICATION TO THE VAN DER POL MODEL OF LASER THRESHOLD

As a two-dimensional example, we consider the rotating Van der Pol oscillator, a popular simple model for the laser threshold[6]. The Fokker-Planck equation now describes the evolution of the quasiprobability P-function $P(\alpha,\alpha^*,t)$ in the interaction picture

$$\frac{\partial}{\partial t}P(\alpha,\alpha^*,t) = \left\{-\frac{\partial}{\partial\alpha}\left[\left(g-|\alpha|^2\right)\alpha\right] - \frac{\partial}{\partial\alpha^*}\left[\left(g-|\alpha|^2\right)\alpha^*\right] + 4\frac{\partial^2}{\partial\alpha\partial\alpha^*}\right\}P(\alpha,\alpha^*,t)\,. \tag{11}$$

In Eq. (11) the complex field amplitude α and the time t have been rescaled in order to have only the free parameter g (g is a pumping parameter, $g = 0$ corresponds to the threshold). As the diffusion matrix is constant positive, for initial positive definite $P(\alpha,\alpha^*,0)$—for example, a coherent state, i. e. a delta-like $P(\alpha,\alpha^*,0)$—the probability distribution remains positive for all times. Moreover, contrarily to the previous example, here it is not necessary to impose particular boundary conditions (α is defined in the whole complex plane)

In Fig. 3 a sample of the probability distribution in the α-plane along with the respective number probability distribution is given for fixed g and three different times,

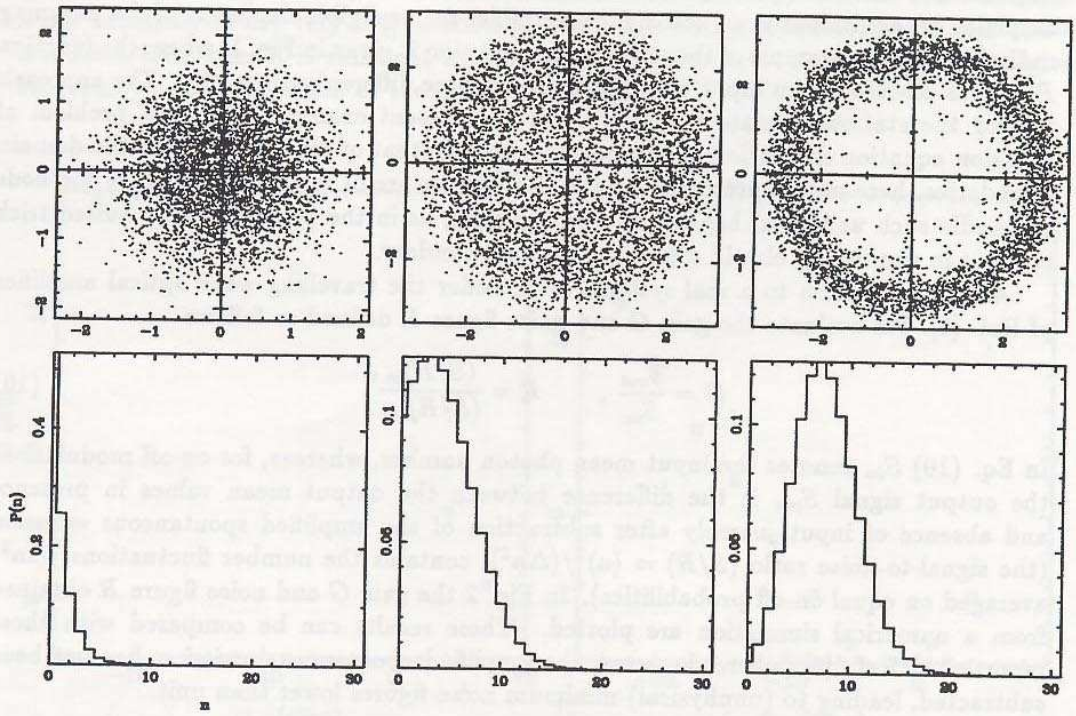

Figure 3: α-plane representation of the P-function and number probability distribution for the Van der Pol equation (11) with initial vacuum state, $g = 8$ and three different times $t = 1/10, 1/4, 1/2$.

starting from radiation in the vacuum state ($P(\alpha, \alpha^*, 0) = \delta_2(\alpha)$ is equivalent to diffusing just the zero point). Notice that the evolution of the field is isotropic in the α-plane, as expected from Eq. (11). The number probability distribution is obtained according to the Fourier transform

$$p(n,t) = \int_{-\infty}^{+\infty} \frac{dx}{2\pi} e^{-inx} \int d^2\alpha P(\alpha, \alpha^*, t) e^{|\alpha|^2(e^{ix}-1)} . \tag{12}$$

As a test of the method, in Fig. 4 the simulation steady-state result ($t = t_s \to \infty$) for both the average $\langle \hat{n} \rangle$ and the Fano factor $F = \langle \Delta \hat{n}^2 \rangle / \langle \hat{n} \rangle$ is compared with the analytical result which follows from the normal-ordered moments

$$\langle \hat{n} \rangle_{t=t_s} = g + \frac{2}{\sqrt{\pi}} \frac{\exp(-g^2/4)}{1 + \Phi(g/2)} , \tag{13}$$

$$\langle a^{\dagger 2} a^2 \rangle_{t=t_s} = g^2 + 2 + g \frac{2}{\sqrt{\pi}} \frac{\exp(-g^2/4)}{1 + \Phi(g/2)} . \tag{14}$$

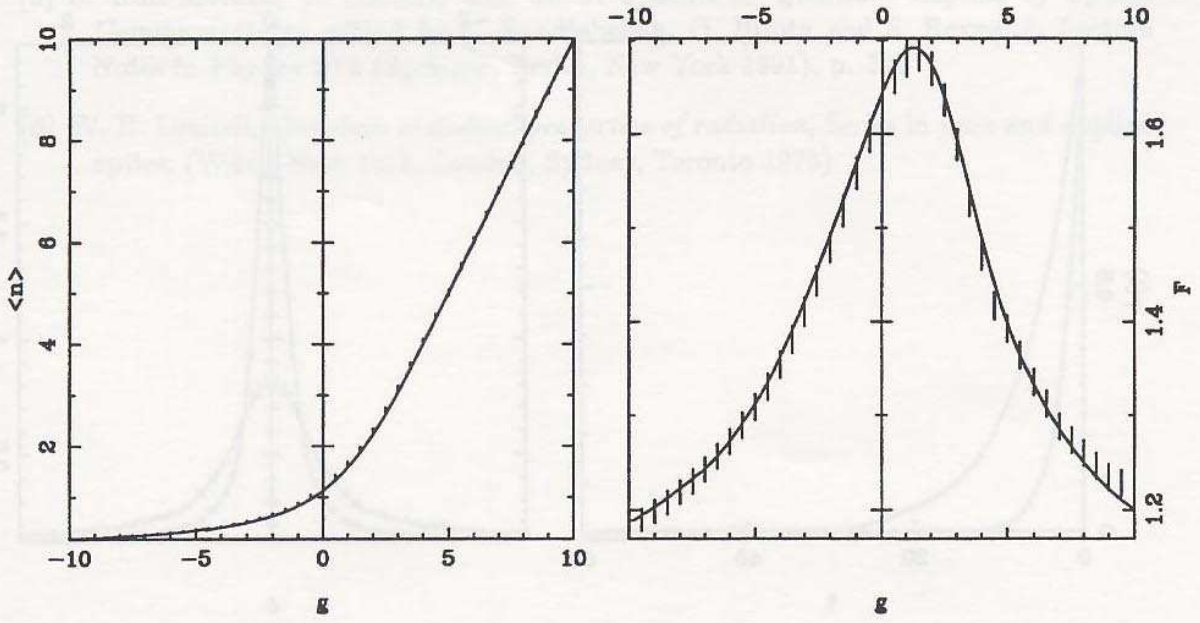

Figure 4: Van der Pol equation (11): steady-state average $\langle \hat{n} \rangle$ and Fano factor F versus the pumping parameter g, in comparison with the analytical results

where $\Phi(x)$ denotes the usual erf-function, and the moments are evaluated according to

$$\langle a^{\dagger m} a^n \rangle \equiv \int d^2\alpha P(\alpha, \alpha^*) \alpha^{*m} \alpha^n \; . \tag{15}$$

Finally, in Fig. 5 the field fluctuations are plotted for two different values of g, after the steady state has been reached. The field correlation function is given by

$$\langle a^\dagger(t+t_s) a(t_s) \rangle = \frac{1}{\langle \hat{n}(t_s) \rangle} \sum_{i=1}^{N} \alpha_i^*(t+t_s) \alpha_i(t_s) \; . \tag{16}$$

The imaginary part of $\langle a^\dagger(t+t_s) a(t_s) \rangle$ is vanishing, as a consequence of the isotropic diffusion. The fluctuation spectrum in Fig. 5 is obtained by Fourier transforming the correlation function. In order to estimate in a self-consistent way the error-bars for the spectrum, the statistical ensemble has been divided into many sub-ensembles, evaluating the statistics on the set of Fourier transforms of each sub-ensemble (notice that the high frequency part of the spectrum has been cut off, as it only would exhibit nonphysical oscillations due to statistical fluctuations at short times).

In conclusion, the present simulation approach is suited to the analysis of quantum optical systems, in particular for multidimensional modelling, where the evaluation of

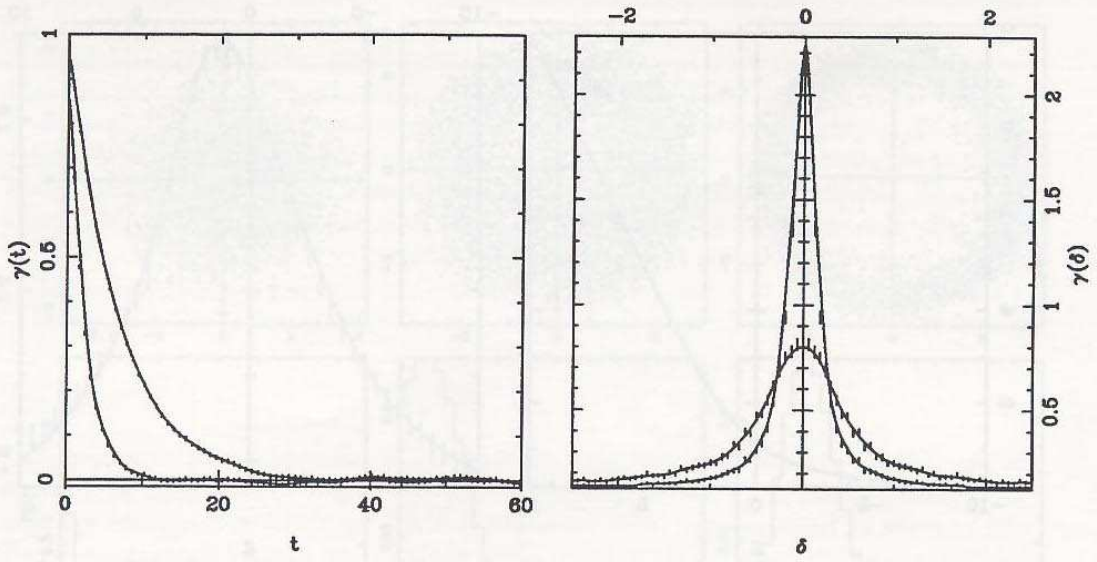

Figure 5: Field correlation functions and corresponding lineshape for $g = 3, 7$ (the same model as in Fig. 4). The full lines are fits of the simulation points.

the physical quantities of interest by direct-integration algorithms becomes prohibitive (but the method maybe conveniently used also for one-dimensional models). This Monte Carlo Green-function method—which is essentially equivalent to a Langevin approach with a locally-Gaussian noise—is a valid simulation technique for the high photon-numbers regime, in alternative to the Monte Carlo wave function simulation of the master equation[1], which can be profitably adopted in the opposite low photon-numbers case.

REFERENCES

[1] C. W. Gardiner, A. S. Parkins, and P. Zoller, Phys. Rev. A **46** 4363 (1992) (and references therein)

[2] L. A. Lugiato, F. Casagrande and L. Pizzuto, Phys. Rev. A **26** 3438 (1982)

[3] S. E. Koonin and D. C. Meredith, *Computational Physics*, (Addison-Wesley, Redwood City, 1990)

[4] P. Meystre and M. Sargent III", *Elements of quantum optics*, Springer-Verlag, Berlin, Heidelberg, New York (1991)

[5] S. Ruiz-Moreno, J. Guitart, and M. J. Soneira in *Quantum Aspects of Optical Communications*, edited by C. Bendjaballah, O. Hirota and S. Reynaud, Lecture Notes in Physics **378** (Springer, Berlin, New York 1991), p. 376

[6] W. H. Louisell, *Quantum statistical properties of radiation*, Series in pure and applied optics, (Wiley, New York, London, Sydney, Toronto 1973)